JOURNAL OF AGRICULTURAL AND FOOD CHEMISTRY

LDL-Antioxidant Pterocarpans from Roots of *Glycine max* (L.) Merr.

JIN HWAN LEE,† BYONG WON LEE,† JIN HYO KIM,† TAE-SOOK JEONG,‡ MIN JUNG KIM,‡ WOO SONG LEE,‡ AND KI HUN PARK*,†

Division of Applied Life Science (BK21 Program), Department of Agricultural Chemistry, Institute of Agriculture and Life Science, Gyeongsang National University, Jinju 660-701, Korea, and National Research Laboratory of Lipid Metabolism and Atherosclerosis, Korea Research Institute of Bioscience and Biotechnology, Daejeon 305-333, Korea

The methanolic root extract of *Glycine max* (L.) Merr. was chromatographed, which yielded 10 flavonoids, including three isoflavones **1**−**3**, five pterocarpans **4**−**8**, one flavonol **9**, and one anthocyanidin **10**. All isolated compounds were examined for LDL-antioxidant activities using four different assay systems on the basis of Cu^{2+}-mediated oxidation. Among them, seven compounds showed potent LDL-antioxidant activities in the thiobarbituric acid reactive substances (TBARS) assay, the lag time of conjugated diene formation, relative electrophoretic mobility (REM), and fragmentation of apoB-100 on copper-mediated LDL oxidation. Three pterocarpans **4**, **6**, and **7**, never reported as LDL-antioxidant, showed potent activities with IC_{50} values of 19.8, 0.9, 45.0 μM, respectively, in comparison with probucol (IC_{50} = 5.6 μM) as positive control. Interestingly, coumestrol **6** (IC_{50} = 0.9 μM) showed 20 times more activity in the TBARS assay than genistein (IC_{50} = 30.1 μM) and daidzein (IC_{50} = 21.6 μM), representative antioxidants in soybean. Moreover, coumestrol **6** had an extended lag time of 190 min at 3.0 μM in measuring conjugated diene formation, while both genistein (120 min) and daidzein (93 min) lag times were extended to less than 120 min at the same concentration.

KEYWORDS: ***Glycine max*** **(L.) Merr. roots; LDL-antioxidation; atherosclerosis; pterocarpan; coumestrol**

INTRODUCTION

Soybeans or soy products have had unprecedented attention due to their potential beneficial effects on various chronic diseases such as cancer, coronary heart disease, osteoporosis, and menopausal discomfort (*1*−*6*). Due to lower rates of heart disease and the association of cancer with higher intakes of soy products, soy has been subjected to extensive investigation regarding its bioactive function. It is well established that flavonoids are responsible for the antioxidant activity of soy (*7*, *8*). Even though there are more than 30 valuable flavonoids in soybean, researchers mainly have focused on three representative isoflavones: genistein, daidzein, and glycitein (*9*−*11*). It is generally accepted that roots contain more abundant secondary metabolites than other parts of the plant, but the elucidation of the biologically active substance from soybean roots has not been studied extensively. Moreover, the earlier reports on roots were based on the analyses using HPLC (*12*) and not isolated by silica gel column chromatography. Thus, evaluation of a biological function of other isoflavones in soybean and its roots are of great importance to enhance not only the value of roots as functional materials but also that of soybean as dietary supplement. Recently, we found that pterocarpans from roots of *Glycine max* (L.) Merr. showed a potent low-density lipoprotein (LDL) oxidation inhibitory activity similar to the three representative isoflavones described above (*7*).

The oxidative modification of LDL plays a considerable role in the early atherosclerosis process (*13*, *14*). When LDL is oxidized, it is modified in several ways through the reaction with reactive oxygen species (ROS), and the oxidized LDL within arterial walls promotes several steps in atherosclerosis (*13*), including endothelial cell damage (*15*, *16*), foam cell accumulation (*17*, *18*), and growth (*19*, *20*) and synthesis of autoantibodies (*21*). Moreover, oxidized LDL promotes monocytes to cause expression of adhesion molecules on the cell surface (*22*). Monocyte-derived macrophages recognize oxidized LDL through the scavenger receptor, resulting in the massive accumulation of lipids (*23*).

In this study, we isolated 10 flavonoids from the roots of *G. max* and identified their structures through spectroscopic methods (see **Figure 1**). Isolated compounds were also evaluated for their inhibitory activity on copper-induced LDL oxidation through four methods: thiobarbituric acid reactive substances (TBARS) assay (*24*), measurement of the formation of conjugated diene (*25*), relative electrophoretic mobility (REM) (*26*), and fragmentation of apoB-100 (*27*).

* Corresponding author. Phone: +82-55-751-5472. Fax: +82-55-757-0178. E-mail: khpark@gsnu.ac.kr.
† Gyeongsang National University.
‡ Korea Research Institute of Bioscience and Biotechnology.

10.1021/jf052431c CCC: $33.50
Published on Web 03/01/2006

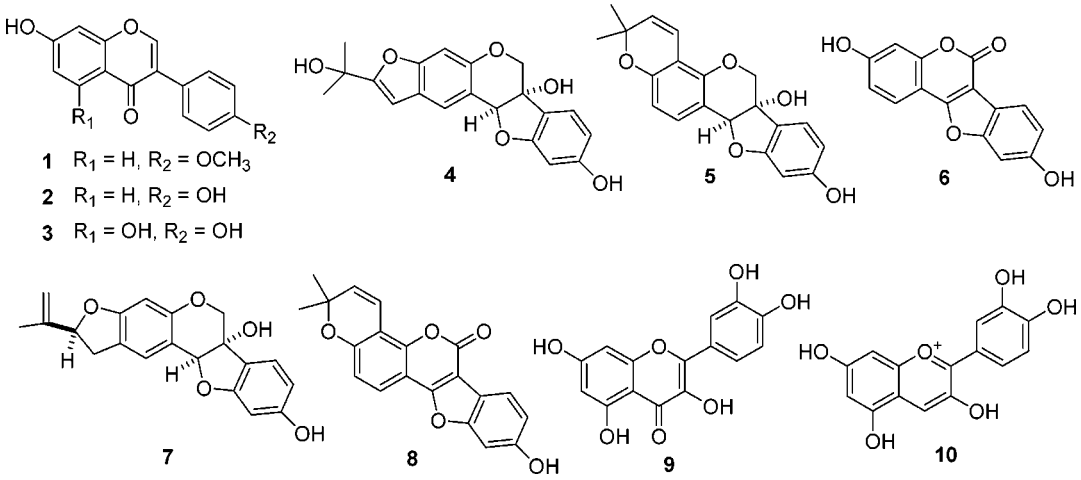

Figure 1. Chemical structures of isolated compounds **1**–**10** in roots of *Glycine max* (L.) Merr.

MATERIALS AND METHODS

Plant Material. The roots of *G. max* (Taekwangkong) were collected on 10 days after R8 at Moonsan, Jinju, Korea at the end of September 2003. The fresh roots of *G. max* were then dried.

General Apparatus and Chemicals. All purifications were monitored by TLC (E. Merck Co., Darmstadt, Germany) using commercially available glass-backed plates and visualized under UV at 254 and 366 nm or sprayed with *p*-anisaldehyde solution. Column chromatography was carried out using 230−400 mesh silica gel (kieselgel 60, Merck, Germany). Melting points were measured on a Thomas Scientific capillary melting point apparatus (Electrothermal 9300, U.K.) and are uncorrected. IR spectra were recorded on a Bruker IFS66 (Bruker, Karlsruhe, Germany) infrared Fourier transform spectrophotometer (KBr), and UV spectra were measured on a Beckman DU650 spectrophotometer (Beckman Coulter, Fullerton, CA). ^{1}H and ^{13}C NMR along with 2D NMR data were obtained on a Bruker AM 500 (^{1}H NMR at 500 MHz, ^{13}C NMR at 125 MHz) spectrometer (Bruker, Karlsruhe, Germany) in $CDCl_3$, acetone-d_6, DMSO-d_6, and CD_3OD. EIMS was obtained on a JEOL JMS-700 mass spectrometer (JEOL, Tokyo, Japan). All the reagent grade chemicals were purchased from Sigma (Sigma Chemical Co, St. Louis, MO).

Extraction and Isolation. The roots (2.4 kg) of *G. max* were air-dried, chopped, and extracted three times with methanol (12 L × 3) for 10 days at room temperature. The combined methanol extract was concentrated in vacuo to yield a green gum (120 g). The methanol extract was dissolved in 1.2 L of a mixture of water and methanol (3:1) and successively partitioned with EtOAc and BuOH (each 3 × 1.2 L), yielding an EtOAc extract (42.4 g), a BuOH extract (20.9 g), and a H_2O extract (48.6 g). The EtOAc phase was chromatographed on silica gel (7 × 60 cm, 230−400 mesh, 850 g) using hexane/acetone [20:1 (1.2 L), 15:1 (1.2 L), 10:1 (1.2 L), 5:1 (1.2 L), 1:1 (1.2 L)] and $CHCl_3$/MeOH [10:1 (1.2 L), 6:1 (1.2 L), 3:1 (1.2 L), 1:1 (1.2 L)] mixtures to give fraction A (14.2 g), fraction B (6.5 g), fraction C (3.5 g), fraction D (1.3 g), fraction E (2.7 g), fraction F (3.0 g), and fraction G (5.9 g). Fraction B was applied to a silica gel column (5 × 50 cm, 230−400 mesh, 220 g) and chromatographed with hexane/acetone (30:1 → 2:1) to afford 60 subfractions; subfractions 39−52 were subjected to silica gel column (3 × 60 cm, 230−400 mesh, 170 g) chromatography with hexane/acetone (12:1 → 4:1) to yield compounds **1** (24 mg) and **8** (12 mg). Fraction C was subjected to silica gel column (4 × 65 cm, 230−400 mesh, 200 g) chromatography with hexane/acetone (10:1 → 1:2) and then purified by a second flash silica gel column (3 × 50 cm, 230−400 mesh, 150 g) using a gradient of hexane/acetone [8:1 (500 mL), 6:1 (350 mL), 4:1 (250 mL), 2:1 (250 mL), 1:1 (250 mL), 1:2 (250 mL)] to yield compounds **2** (18 mg) and **3** (32 mg). Fraction D was submitted to silica gel column (2.5 × 60 cm, 230−400 mesh, 130 g) chromatography and eluted with a $CHCl_3$/acetone gradient (25:1 → 4:1) resulting in 55 subfractions; subfractions 39−47 were rechromatographed on silica gel with $CHCl_3$/acetone (12:1 → 2:1) to yield compounds **4** (69 mg) and **5** (45 mg). Fraction E was chromatographed using a stepwise gradient of $CHCl_3$/acetone [15:1 (500 mL), 12:1 (400 mL), 8:1 (400 mL), 5:1 (400 mL), 2:1 (400 mL), 1:1 (400 mL)], then purified by second flash silica gel column (2.0 × 50 cm, 230−400 mesh, 100 g) using a gradient of $CHCl_3$/acetone [10:1 (250 mL), 6:1 (180 mL), 3:1 (180 mL), 2:1 (180 mL), 1:1 (180 mL)] to yield compounds **6** (58 mg) and **7** (21 mg). The BuOH phase was chromatographed on silica gel (4.5 × 60 cm, 230−400 mesh, 650 g) using a gradient of $CHCl_3$/MeOH [30:1 (1.0 L), 20:1 (1.0 L), 15:1 (1.0 L), 10:1 (1.0 L), 6:1 (1.0 L), 3:1 (1.0 L), 1:1 (1.0 L)] to give fractions A−F. Fraction D (940 mg) was repeatedly chromatographed over silica gel (2.5 × 60 cm, 230−400 mesh, 130 g) using $CHCl_3$/MeOH [15:1 (400 mL), 10:1 (200 mL), 6:1 (200 mL), 3:1 (200 mL), 1:1 (200 mL)] to yield compound **9** (42 mg), and fraction E (220 mg) was separately subjected to silica gel column (1.5 × 30 cm, 230−400 mesh, 40 g) chromatography with the same solvent [10:1 (100 mL), 6:1 (80 mL), 3:1 (80 mL), 1:1 (80 mL)] used for **9** and rechromatographed on a Sephadex LH-20 (1.0 × 50 cm) and a C_{18} column for elution with methanol in order to yield compound **10** (29 mg).

Compound Identification. The structures of isolated compounds **1**−**3** were confirmed by spectroscopic analysis and comparison with values previously reported (*28*−*30*). Herein, we report ^{13}C NMR spectroscopic data.

Glyceofuran (4): colorless needles; mp 181−183 °C [lit. mp 181 °C (dec)] (*31*); EIMS *m*/*z* (relative intensity) 354 (M^+, 25%), 339 (100%), 336 (36%); IR (KBr) ν_{max} 3414, 1660, 1555 cm^{-1}; UV λ_{max} nm 306, 293, 287, 250, 226 (EtOH); ^{1}H NMR (500 MHz, CD_3OD) δ 1.60 (6H, s, 15-CH_3 and 16-CH_3), 3.98 (1H, d, J = 11.4 Hz, H-6β), 4.16 (1H, d, J = 11.4 Hz, H-6α), 5.37 (1H, s, H-11a), 6.23 (1H, d, J = 2.1 Hz, H-10), 6.42 (1H, dd, J = 8.2, 2.1 Hz, H-8), 6.60 (1H, d, J = 0.6 Hz, H-12), 6.97 (1H, s, H-4), 7.18 (1H, d, J = 8.2 Hz, H-7), and 7.63 (1H, s, H-1). ^{13}C NMR (125 MHz, CD_3OD): see **Table 1**.

Glyceollin I (5): amorphous yellow powder; mp 102−104 °C; EIMS *m*/*z* (relative intensity) 338 (M^+, 22%), 323 (100%), 321 (38%), 280 (6%); IR (KBr) ν_{max} 3460, 1860, 1650 cm^{-1}; UV λ_{max} nm 350, 298, 280, 262, 230 (EtOH) (*31*); ^{1}H NMR (500 MHz, CD_3Cl) δ 1.36 (3H, s, 15-CH_3), 1.39 (3H, s, 16-CH_3), 3.95 (1H, d, J = 6.9 Hz, H-6α), 4.15 (1H, d, J = 6.9 Hz, H-6β), 5.18 (1H, s, H-11a), 5.52 (1H, d, J = 10.0 Hz, H-13), 6.23 (1H, s, H-10), 6.29 (1H, d, J = 8.1 Hz, H-8), 6.49 (1H, d, J = 8.4 Hz, H-2), 6.55 (1H, d, J = 10.0 Hz, H-12), 7.05 (1H, d, J = 8.1 Hz, H-7), and 7.15 (1H, d, J = 8.4 Hz, H-1). ^{13}C NMR (125 MHz, CD_3Cl): see **Table 1**.

Coumestrol (6): yellow needles; mp 355−359 °C [lit. mp 360−365 °C (dec)] (*32*); EIMS *m*/*z* (relative intensity) 268 (M^+, 100%), 240 (15%), 211 (9%), 280 (6%); IR (KBr) ν_{max} 3500, 2820, 1710 cm^{-1}; UV λ_{max} nm 378, 310, 280, 210 (MeOH); ^{1}H NMR (500 MHz, DMSO-d_6) δ 6.92 (1H, d, J = 2.2 Hz, H-4), 6.94 (1H, dd, J = 8.5, 2.1 Hz, H-2), 6.96 (1H, dd, J = 8.3, 2.1 Hz, H-8), 7.18 (1H, d, J = 2.0 Hz,

Table 1. ^{13}C NMR of Compounds **1**–**10** at 125 MHz (ppm, m)[a]

	compound									
position	**1**	**2**	**3**	**4**	**5**	**6**	**7**	**8**	**9**	**10**
1				124.5 d	131.3 d	123.1 d	127.8 d	121.9 d		
2	153.5 d	153.2 d	154.3 d	125.4 s	111.5 d	114.2 d	121.8 s	114.1 d	147. 1 s	162.5 s
3	123.5 s	123.9 s	121.6 s	157.2 s	154.4 s	161.6 s	145.3 s	155.7 s	136.0 s	146.6 s
4	175.0 s	175.1 s	180.6 s	99.4 d	110.7 s	103.4 d	98.2 d	109.6 s	176.1 s	134.2 d
4a	117.0 s	117.0 s	104.8 s	154.5 s	150.7 s	155.0 s	156.5 s	148.9 s		113.7 s
5	127.6 d	127.7 d	162.4 s						160.8 s	158.2 s
6	115.6 d	115.6 d	99.3 d	72.1 t	70.1 t	158.0 s	70.8 t	157.6 s	98.5 d	103.2 d
6a				78.0 s	77.1 s	102.4 s	76.8 s	103.0 s		
6b				121.6 s	120.3 s	115.0 s	121.5 s	114.8 s		
7	163.0 s	163.1 s	164.7 s	125.6 s	124.6 d	121.0 d	125.2 d	121.2 d	164.1 s	169.4 s
8	102.5 d	102.5 d	94.0 d	109.9 d	109.2 d	114.4 d	109.0 d	114.5 d	93.7 d	94.9 d
8a	157.8 s	157.9 s	158.0 s							
9				161.6 s	161.1 s	156.3 s	162.0 s	156.4 s	156.5 s	
10				99.3 d	99.2 d	99.1 d	98.6 d	99.1 s	103.3 s	
10a				162.7 s	158.8 s	157.4 s	160.7 s	157.5 s		
11										
11a				87.2 d	85.5 d	160.0 s	86.4 d	159.6 s		
11b				118.8 s	112.7 s	104.5 s	112.0 s	106.1 s		
12				101.4 d	116.8 d		34.4 t	114.7 d		
13				165.7 s	129.8 d		87.3 d	132.4 d		
14				70.1 s	76.8 s		162.0 s	78.1 s		
15							114.0 t			
$15CH_3$				29.3 q	28.2 q			28.2 q		
$16CH_3$				29.3 q	28.2 q		17.3 q	28.2 q		
1′	124.6 s	123.0 s	122.7 s						122.3 s	122.0 s
2′	130.4 d	130.5 d	130.5 d						115.4 d	118.1 d
3′	114.0 d	115.4 d	115.4 d						145.3 s	147.5 s
4′	159.3 s	157.6 s	157.8 s						147.9 s	155.3 s
5′	114.0 d	115.4 d	115.4 d						115.9 d	117.4 d
6′	130.4 d	130.5 d	130.5 d						120.3 d	127.3 d
OCH_3	55.5 q									

[a] The chemical shifts of compound **7** were determined in acetone-d_6, compounds **1**–**3**, **6**, **8**, and **9** were measured in DMSO-d_6, and compound **5** was measured in $CDCl_3$. Compounds **4** and **10** were measured in CD_3OD.

H-10), 7.71 (1H, d, J = 8.4 Hz, H-7), and 7.87 (1H, d, J = 8.6 Hz, H-1). ^{13}C NMR (125 MHz, DMSO-d_6): see **Table 1**.

Glyceollin III (7): colorless needles; mp 149−154 °C; EIMS *m*/*z* (relative intensity) 338 (M^+, 15%), 323 (100%), 297 (32%); IR (KBr) ν_{max} 3414, 1660, 1555 cm^{-1}; UV λ_{max} nm 306, 293, 287, 250, 226 (EtOH); (*29*, *33*) ^1H NMR (500 MHz, acetone-d_6) δ 1.74 (3H, s, 16-CH_3), 3.01 (1H, m, H-12β), 3.33 (1H, m, H-12α), 4.02 (1H, d, J = 11.3 Hz, H-6β), 4.12 (1H, d, J = 11.3 Hz, H-6α), 4.88 (1H, m, 15α), 5.05 (1H, m, 15β), 5.24 (1H, t, J = 8.5 Hz, H-13), 5.27 (1H, s, H-11a), 6.24 (1H, s, H-10a), 6.25 (1H, s, H-4), 6.44 (1H, dd, J = 8.2, 2.1 Hz, H-8), 7.20 (1H, d, J = 8.1 Hz, H-7), and 7.24 (1H, s, H-1). ^{13}C NMR (125 MHz, acetone-d_6): see **Table 1**.

Plicadin (8): yellow solid; mp 127−129 °C [lit. mp 127 °C, 289−290 °C] (*34*, *35*); EIMS *m*/*z* (relative intensity) 334 (M^+, 24%), 319 (100%), 318 (6%); IR (KBr) ν_{max} 3341, 1750, 1640, 1600, 1522 cm^{-1}; UV λ_{max} nm 364, 351, 302, 224 (MeOH); ^1H NMR (500 MHz, DMSO-d_6) δ 1.47 (6H, s, 15-CH_3 and 16-CH_3), 6.00 (1H, d, J = 10.1 Hz, H-13), 6.85 (1H, d, J = 10.1 Hz, H-12), 6.94 (1H, d, J = 8.6 Hz, H-2), 6.98 (1H, dd, J = 8.3, 1.8 Hz, H-8), 7.19 (1H, d, J = 2.0 Hz, H-10), 7.74 (1H, d, J = 8.4 Hz, H-7), and 7.80 (1H, d, J = 8.6 Hz, H-1). ^{13}C NMR (125 MHz, DMSO-d_6): see **Table 1**.

Quercetin (9): yellow powder; mp 282−285 °C [lit. mp 300−302 °C] (*36*); EIMS *m*/*z* (relative intensity) 302 (M^+, 100%), 273 (7%), 153 (3%), 137 (3%); IR (KBr) ν_{max} 3407, 1665, 1662, 1519 cm^{-1}; UV λ_{max} nm 382, 353, 274 (MeOH); ^1H NMR (500 MHz, DMSO-d_6) δ 6.21 (1H, d, J = 1.8 Hz, H-6), 6.43 (1H, d, J = 1.8 Hz, H-8), 6.90 (1H, d, J = 8.5 Hz, H-5′), 7.56 (1H, dd, J = 8.5, 2.1 Hz, H-6′), and 7.69 (1H, d, J = 2.1 Hz, H-2′). ^{13}C NMR (125 MHz, DMSO-d_6): see **Table 1**.

Cyanidin (10): dark red powder; mp 228−230 °C [lit. mp 194−195 °C] (*37*); EIMS *m*/*z* (relative intensity) 287 (M^+, 7%); IR (KBr) ν_{max} 3425, 3187, 2918, 2860 cm^{-1}; UV λ_{max} nm 476, 380, 364, 303, 278 (MeOH); ^1H NMR (500 MHz, CD_3OD) δ 6.62 (1H, d, J = 1.6 Hz, H-6), 6.86 (1H, s, H-8), 7.00 (1H, d, J = 8.7 Hz, H-5′), 8.10 (1H, d, J = 2.3 Hz, H-2′), 8.21 (1H, dd, J = 8.7, 2.3 Hz, H-6′), and 8.56 (1H, s, H-4). ^{13}C NMR (125 MHz, CD_3OD): see **Table 1**.

Isolation of LDL. The blood was obtained from healthy volunteers. EDTA was used as anticoagulant (1.5 mg/mL of blood). After low-speed centrifugation of the whole blood to obtain plasma and to prevent lipoprotein modification, 0.1% EDTA, 0.05% NaN_3, and 0.015% PMSF (phenylmethanesulfonyl fluoride) were added. LDL (1.019−1.063 g/mL) was isolated from the plasma by sequential density ultracentrifugation at 4 °C in a Beckman TL ultracentrifuge (Beckman Instruments, Mountain View, CA) as described previously (*38*). After the isolation, LDL was dialyzed overnight against three changes of phosphate buffer (pH 7.4), containing 150 mM NaCl, in the dark at 4 °C to remove EDTA. The LDL in phosphate-buffered saline (PBS) was stored at 4 °C and used within 4 weeks.

LDL Oxidation. LDL (120 μg protein/mL) was diluted in PBS buffer (10 mM, pH 7.4). Oxidation was initiated by adding freshly prepared 5 μM $CuSO_4$, and the reaction was stopped by adding of 1 mM EDTA. In our experiments, oxidation was carried out in the presence or absence of compounds. After incubation, TBARS, conjugated diene, REM, and ApoB-100 fragmentation of LDL were measured as described below. Probucol, a known antioxidant having antiatherogenic activity, was used as a positive control substance in a series of experiments.

Thiobarbituric Acid Reactive Substances (TBARS). The formation of TBARS assay of Buege and Aust (*24*) was used with minor modifications. Briefly, the LDL solution (250 μL, 120 μg of protein) in PBS (10 mM, pH 7.4, 0.15 M NaCl) was supplemented with 10 μM $CuSO_4$. The oxidation was performed in a screw-capped 5 mL glass vial at 37 °C in a shaking water bath. After 4 h of incubation, the reaction was terminated by addition of 1 mL of 20% trichloroacetic acid. Following precipitation, 1 mL of 0.67% TBA in 0.05 N NaOH was added and vortexed, and then the final mixture was heated for 5

min at 95 °C, cooled on ice, and centrifuged for 2 min at 1000*g*. The optical density of the produced malondialdehyde (MDA) was measured at 532 nm.

Conjugated Diene Formation. The formation of conjugated diene was measured by monitoring the absorbance at 234 nm using the method of Esterbauer et al. (*25*). Briefly, LDL (120 μg/mL), in PBS (pH 7.4) was incubated with 5 μM $CuSO_4$ solution, in the presence or absence of test compounds, at 37 °C, for 4 h; thereafter, the absorbance at 234 nm was measured every 10 min. The plot of absorbance against time produces three phase: (1) a lag phase, (2) a propagation phase, and (3) a decomposition phase. The lag time (the extent to which the compounds protected LDL from oxidation was reflected by the prolongation of the lag phase compared to that of the control) was measured as the intercept between the baseline and the tangent of the absorbance curve during the propagation phase.

Relative Electrophoretic Mobility (REM). The electrophoretic mobility of native or oxidized LDL was detected by agarose gel electrophoresis (Ciba Corning Diagnostics, Palo Alto, CA) using the method of Reid and Mitchinson (*26*). The LDL (120 μg/mL) in PBS (pH 7.4) was oxidized with 5 μM $CuSO_4$ for 12 h at 37 °C with or without compounds. Thereafter, the agarose gel (0.7% agarose) was electrophoresed (85 V) in a buffer containing 40 mM Tris, 40 mM glacial acetic acid, and 1 mM EDTA for 1 h. After electrophoresis, lipoprotein bands were stained with coomassie brilliant blue; REM was defined as the ratio of the migrating distance of oxidized LDL to that of the control.

Electrophoresis of ApoB-100 Fragmentation. The electrophoresis of apoB-100 fragmentation was performed according to the procedures of Noguchi and Niki (*27*). Briefly, after the oxidation with or without antioxidants, samples were denatured with 3% SDS, 10% glycerol, and 5% 2-mercaptoethanol at 95 °C for 10 min. SDS−polyacrylamide gel electrophoresis (SDS−PAGE, 3−15% gradient) was performed to detect the apoB-100 fragmentation. The electrophoresis was processed at 48 V for 150 min. After the electrophoresis, the gel was dried and stained with coomassie brilliant blue R250 and subjected to densitometric scanning by a Bio Rad model GS-800 with Bio Rad Quantity One-4.4.0 software.

RESULTS AND DISCUSSION

Repeated silica gel chromatography of the methanolic root extract of *G. max* and recrystallization yielded 10 flavonoids, which were identified as three isoflavones **1**−**3**, five pterocarpans **4**−**8**, one flavonol **9**, and one anthocyanidin **10**. The physical and spectroscopic data of the isolated compounds showed identity with those of formononetin (**1**), daidzein (**2**), genistein (**3**), glyceofuran (**4**), glyceollin I (**5**), coumestrol (**6**), glyceollin III (**7**), plicadin (**8**), quercetin (**9**), and cyanidin (**10**). Among them, this is the first report on the isolation of plicadin **8** from this plant. The 10 isolated flavonoids were evaluated for their inhibitory activity on Cu^{2+}-induced LDL oxidation by four systems in vitro: the thiobarbituric acid reactive substances (TBARS) assay, a lag time of conjugated diene formation, the relative electrophoretic mobility (REM), and the fragmentation of apoB-100. As a result, seven flavonoids **2**−**4**, **6**, **7**, **9**, and **10** showed potent LDL-antioxidant activities. The ability of isolated compounds **1**−**10** to attenuate Cu^{2+}-induced LDL oxidation was measured by the TBARS assay. As shown in **Table 2**, compounds **2**−**4**, **6**, **7**, **9**, and **10** showed potent antioxidant activities with IC_{50} values of 21.6, 30.1, 19.8, 0.9, 45.0, 5.1, and 44.5 μM, respectively, and probucol, which was used as a positive control, exhibited an IC_{50} value of 5.6 μM. It is well-known that daidzein **2** and genistein **3** have a potent inhibitory effect on LDL oxidation, and antioxidant activity in soybean has been mainly focused on these two compounds. In this study, it was found that pterocarpans **4**, **6**, and **7** had potent LDL-antioxidant properties as constituents of soybean; pterocarpan **6** especially showed 30 times more activity than genistein (IC_{50} = 30.1 μM).

Table 2. Inhibitory Effects of Isolated Compounds **1**–**10** on Cu^{2+}-Mediated LDL Oxidation by Measurement of TBARS Assay

compounds	IC_{50} (μM) values[a]
1	NI
2	21.6
3	30.1
4	19.8
5	NI
6	0.9
7	45.0
8	NI
9	5.1
10	44.5
probucol	5.6

[a] All compounds were examined in triplicate; IC_{50} values of compounds represent the concentration that caused 50% inhibition of LDL antioxidant activity. NI is no inhibition.

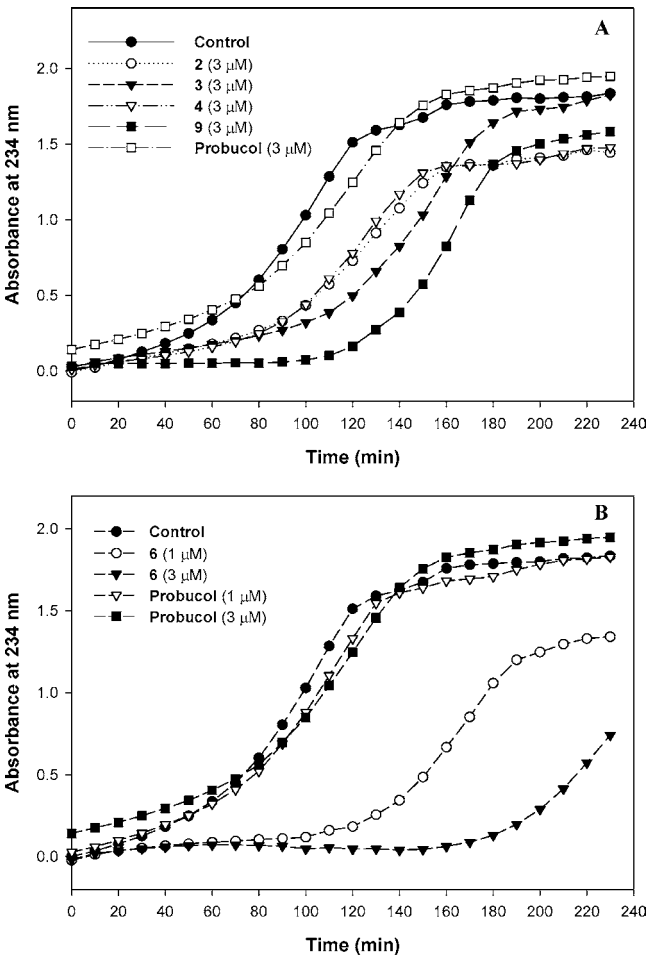

Figure 2. Effects of compounds **2**–**4**, **6**, and **9** on the generation of conjugated diene. Conjugated diene formation was measured by determining the absorbance at 234 nm every 10 min for 4 h. Probucol was used as a reference antioxidant.

On the basis of TBARS assay results, five potent LDL-antioxidants, **2**−**4**, **6**, and **9**, were determined by measuring the conjugated diene formation at 234 nm for 240 min. The lag time of conjugated diene production, indicating the resistance of LDL to oxidation, was prolonged when LDL was incubated with compounds **2**−**4**, **6**, and **9**. As shown in **Figure 2A**, the control LDL (120 μg/mL) incubated with 5 μM $CuSO_4$ had a lag time of 70 min, whereas the lag time was extended to 93 (**2**), 120 (**3**), 88 (**4**), and 130 min (**9**), when treated with each of

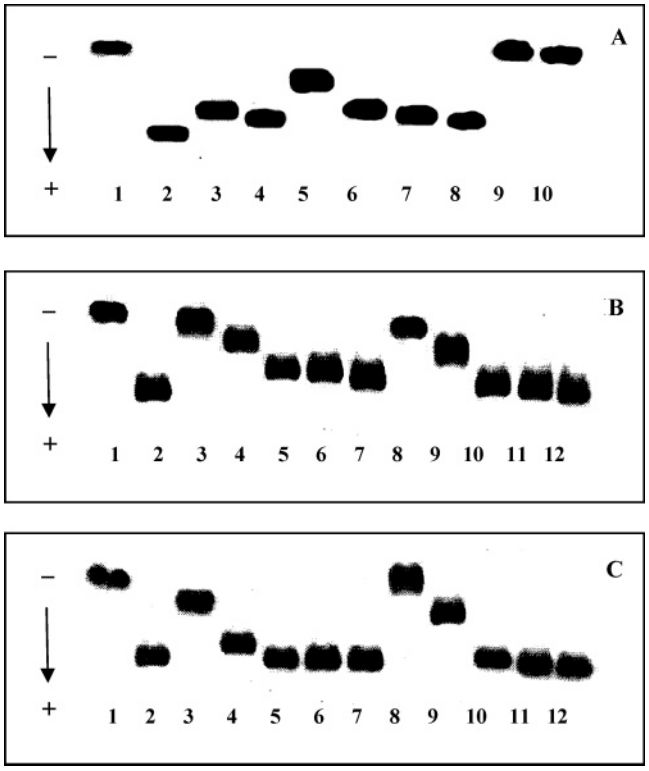

Figure 3. Effects of compounds **2**–**4** (**A**), **6** (**B**), and **9** (**C**) on the Cu^{2+}-mediated oxidation and electrophoretic mobility of LDL. (**A**) Lane 1, native LDL (absence of $CuSO_4$); lane 2, ox-LDL; lane 3, **2** (50 μM); lane 4, **2** (25 μM); lane 5, **3** (50 μM); lane 6, **3** (25 μM); lane 7, **4** (50 μM); lane 8, **4** (25 μM); lane 9, probucol (50 μM); lane 10, probucol (25 μM). (**B**) Lane 1, native LDL (absence of $CuSO_4$); lane 2, ox-LDL; lane 3, **6** (20 μM); lane 4, **6** (10 μM); lane 5, **6** (5 μM); lane 6, **6** (3 μM); lane 7, **6** (1 μM); lane 8, probucol (20 μM); lane 9, probucol (10 μM); lane 10, probucol (5 μM); lane 11, probucol (3 μM); lane 12, probucol (1 μM). (**C**) Lane 1, native LDL (absence of $CuSO_4$); lane 2, ox-LDL; lane 3, **9** (20 μM); lane 4, **9** (10 μM); lane 5, **9** (5 μM); lane 6, **9** (3 μM); lane 7, **9** (1 μM); lane 8, probucol (20 μM); lane 9, probucol (10 μM); lane 10, probucol (5 μM); lane 11, probucol (3 μM); lane 12, probucol (1 μM).

the compounds at 3.0 μM. Pterocarpan **6** extended the lag time to 132 min at 1.0 μM and 190 min at 1.0 μM (**Figure 2B**). These data revealed that pterocarpan **6** extended the a lag time to double that of probucol, which extended the lag time to 82 min at 3.0 μM. As in the TBARS system, compound **6** gave a better result than the flavonoids, daidzein, and genistein.

To understand another parameter that is affected by LDL oxidation, LDL-antioxidants **2**−**4**, **6**, and **9** were applied to the relative electrophoretic mobility (REM) assay system. As shown in **Figure 3**, native LDL in the absence of 5 μM $CuSO_4$ (lane 1) and the 5 μM $CuSO_4$ alone (lane 2) were employed to oxidized LDL for 12 h. When each of the compounds **2**−**4** was treated at 50 and 25 μM, respectively, the mobility of the LDL was reduced moderately (**Figure 3A**). Also, when 50 μM of compounds **2**−**4** were incubated, LDL oxidation was protected by 21%, 57%, and 14%, respectively, compared to that of oxidized LDL. The more active compounds **6** and **9** were carried out at a dose-dependent concentration of Cu^{2+}-mediated oxidation of LDL (**Figure 3**, parts **B** and **C**). Both compounds **6** and **9** reduced the mobility of LDL up to the concentration of 5 μM and inhibited oxidation of LDL by 67% and 63%, respectively. Among them, compound **6** showed more potent antioxidant activity against LDL oxidation than that of probucol to be a positive control.

Table 3. Antioxidant Effects of **2**–**4**, **6**, and **9** on the Cu^{2+}-Mediated Oxidation and ApoB-100 Fragmentation in LDL

compounds (μM)	area (AU/mm)[a]
native LDL	12.95
ox-LDL	0
2	6.68
3	9.48
4	8.80
6	9.40
9	9.26
probucol	12.00

[a] Areas of the peaks of the apoB-100 are expressed as absorbance units per millimeter.

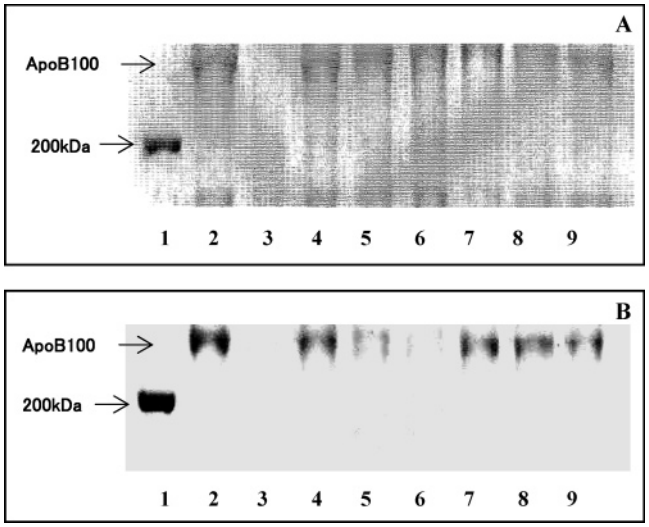

Figure 4. Effects of compounds **6** and **9** on the apoB-100 fragmentation. (**A**) Lane 1, marker; lane 2, native LDL (absence of $CuSO_4$); lane 3, ox-LDL; lane 4, **6** (10 μM); lane 5, **6** (5 μM); lane 6, **6** (1 μM); lane 7, probucol (10 μM); lane 8, probucol (5 μM); lane 9, probucol (1 μM). (**B**) Lane 1, marker; lane 2, native LDL (absence of $CuSO_4$); lane 3, ox-LDL; lane 4, **9** (20 μM); lane 5, **9** (10 μM); lane 6, **9** (5 μM); lane 7, probucol (20 μM); lane 8, probucol (10 μM); lane 9, probucol (5 μM).

Radical reaction of LDL causes fragmentation of apoB-100 which is a major component of LDL. The inhibition of the oxidative process by compounds **2**−**4**, **6**, **9**, and probucol was evaluated also by the fragmentation of apoB-100 through the electrophoretic analysis on 4% polyacrylamide gel in the presence of sodium dodecyl sulfate (SDS−PAGE). The band of apoB-100 was observed on native LDL (120 μg/mL in PBS), which had been incubated without 5 μM $CuSO_4$ for 12 h at 37 °C, but the band completely disappeared when LDL (120 μg/mL in PBS) was incubated with 5 μM $CuSO_4$. As shown in **Table 3**, the densitometric values related to the areas of the peaks of the apoB-100 are expressed as absorbance units per millimeter for the compounds **2**−**4**, **6**, and **9** and probucol at 50 and 10 μM, respectively.

When compounds **2**−**4**, **6**, and **9** were applied to the apoB-100 fragmentation system, compounds **6** and **9** showed a dose-dependent concentration of Cu^{2+}-mediated oxidation of LDL (**Figure 4**). The pterocarpan **6** protected fragmentation of the apoB-100 up to 1 μM (**Figure 4A**), and flavonol **9** was up to 10 μM (**Figure 4B**), whereas daidzein **2** and genistein **3** could not protect the oxidation of the apoB-100 band at 10 μM. The pterocarpan **6** and flavonol **9** were significantly active in the protection of apoB-100 fragmentation against copper-induced oxidation of LDL.

In conclusion, five pterocarpans (**4**−**8**) were isolated, together with five other flavonoids from the roots of *G. max*. Three pterocarpans (**4**, **6**, and **7**) showed potent activities, with IC_{50} value of 19.8, 0.9, and 45.0 μM, respectively in TBARS assay. Interestingly, coumestrol **6** showed 20 times more activity than genistein (IC_{50} = 30.1 μM) and daidzein (IC_{50} = 21.6 μM) in the TBARS assay and extended the lag time to 190 min at 3.0 μM for conjugated diene formation. Thus, the LDL oxidative inhibitory activity of pterocarpans would contribute to enhance the value of soybean and its root as a dietary supplement because both contain all three pterocarpans.

Supporting Information Available: ^{1}H NMR and ^{13}C NMR of compounds **1**−**10**; HMBC NMR of compounds **1** and **3**−**10**; ^{1}H−^{1}H NMR and ^{1}H−^{13}C NMR of compound **6**; EIMS of compounds **6**, **8**, and **9**; and characteristic HPLC chromatogram of isolated compounds **1**−**9**. This material is available free of charge via the Internet at http://pubs.acs.org.

LITERATURE CITED

(1) Wilson, T. A.; Meservey, C. M.; Nicolosi, R. J. Soy lecithin reduces plasma lipoprotein cholesterol and early atherogenesis in hypercholesterolemic monkeys and hamsters: beyond linoleate. *Atherosclerosis* **1998**, *140*, 147−153.

(2) Anthony, M. S.; Clarkson, T. B.; Hughes, C. L.; Morgan, T. M.; Burke, G. L. Soybean isoflavones improve cardiovascular risk factors without affecting the reproductive system of peripubertal Rhesus monkeys. *J. Nutr.* **1996**, *126*, 43−50.

(3) Arjmandi, B. H.; Getlinger, M. J.; Goyal, N. V.; Alekel, L.; Hasler, C. M.; Juma, S.; Drum, M. L.; Hollis, B. W.; Kukreja, S. C. Role of soy protein with normal or reduced isoflavone content in reversing bone loss induced by ovarian hormone deficiency in rats. *Am. J. Clin. Nutr.* **1998**, *68*, 1358S−1363S.

(4) Wu, A. H.; Ziegler, R. G.; Nomura, A. M. Y.; West, D. W.; Kolonel, L. N.; Ross, P. L. H.; Pike, M. C. Soy intake and risk of breast cancer in Asians and Asian Americans. *Am. J. Clin. Nutr.* **1998**, *68*, 1437S−1443S.

(5) Ho, S. C.; Woo, J. L.; Leung, S. S. F.; Sham, A. L. K.; Lam, T. H.; Janus, E. D. Intake of soy products is associated with better plasma lipid profiles in the Hong Kong Chinese population. *J. Nutr.* **2000**, *130*, 2590−2593.

(6) Song, T. T.; Hendrich, S.; Murphy, P. A. Estrogenic activity of glycitein, a soy isoflavone. *J. Agric. Food Chem.* **1999**, *47*, 1607−1610.

(7) Lee, C. H.; Yang, L.; Xu, J. Z.; Yeung, S. Y. V.; Huang, Y.; Chen, Z. Y. Relative antioxidant activity of soybean isoflavones and their glycosides. *Food Chem.* **2005**, *90*, 735−741.

(8) Tikkanen, M. J.; Wahala, K.; Ojala, S.; Vihma, V.; Adlercreutz, H. Effect of soybean phytoestrogen intake on low-density lipoprotein oxidation resistance. *Proc. Natl. Acad. Sci. U.S.A.* **1998**, *95*, 3106−3110.

(9) Wu, Q.; Wang, M.; Sciarappa, W. J.; Simon, J. E. LC/UV/ESI-MS analysis of isoflavones in edamame and tofu soybeans. *J. Agric. Food Chem.* **2004**, *52*, 2763−2769.

(10) Rostagno, M. A.; Palma, M.; Barroso, C. G. Pressurized liquid extraction of isoflavones from soybeans. *Anal. Chim. Acta* **2004**, *522*, 169−177.

(11) Dwyer, J. T.; Goldin, B. R.; Saul, N.; Gualtieri, L.; Barakat, S.; Adlercreutz, H. Tofu and soy drinks contain phytoestrogens. *J. Am. Diet. Assoc.* **1994**, *94*, 739−743.

(12) Porter, P. M.; Banwart, W. L.; Hassett, J. J. HPLC isolation and GC-MS identification of genistein, daidzein, and coumestrol from unhydrolyzed soybean root extracts. *Environ. Exp. Bot.* **1985**, *25*, 229−232.

(13) Steinberg, D.; Pathasarathy, S.; Carew, T. E.; Khoo, J. C.; Witztum, J. L. Beyond cholesterol: modifications of low-density lipoprotein that increase its atherogenicity. *N. Engl. J. Med.* **1989**, *320*, 915−923.

(14) Daugherty, A.; Roselaar, S. E. Lipoprotein oxidation as a mediator of atherogenesis: insights from pharmacological studies. *Cardiovas. Res.* **1995**, *29*, 297−311.

(15) Hessler, I. R.; Morel, D. W.; James, L. J.; Chisolm, G. M. Lipoprotein oxidation and lipoprotein-induced cytotoxicity. *Arteriosclerosis* **1983**, *3*, 215−222.

(16) Yagi, K. Increased serum lipid peroxides initiate atherogenesis. *BioEssays* **1984**, *1*, 58−60.

(17) Quinn, M. T.; Parthasarathy, S.; Steinberg, D. Endothelial cell-derived chemotactic activity for mouse peritoneal macrophages and the effects of modified forms of low-density lipoprotein. *Proc. Natl. Acad. Sci. U.S.A.* **1985**, *82*, 5949−5953.

(18) Gerrity, R. G. The role of the monocyte in atherogenesis: I. Transition of blood-borne monocytes into foam cells in fatty lesions. *Am. J. Pathol.* **1981**, *103*, 181−190.

(19) Fogelman, A. M.; Schechter, I.; Hokom, M.; Child, J. S.; Edwards, P. A. Malondialdehyde alteration of low-density lipoproteins leads to cholesterol ester accumulation in human monocyte-macrophages. *Proc. Natl. Acad. Sci. U.S.A.* **1980**, *77*, 2214−2218.

(20) Goldstein, J. L.; Ho, Y. K.; Basu, S. K.; Brown, M. S. Binding site on macrophages that mediates uptake and degradation of acetylated low-density lipoprotein, producing massive cholesterol deposition. *Proc. Natl. Acad. Sci. U.S.A.* **1979**, *76*, 333−337.

(21) Salonen, J. T.; Ylä-Herttuala, S.; Yamamoto, R.; Butler, S.; Korpela, H.; Salonen, R.; Nyyssönen, K.; Palinski, W.; Witztum, J. L. Autoantibody against oxidized LDL and progression of carotid atherosclerosis. *Lancet* **1992**, *339*, 883−887.

(22) Liao, L.; Starzyk, R. M.; Granger, D. N. Molecular determinants of oxidized low-density lipoprotein-induced leukocyte adhesion and microvascular dysfunction. *Arterioscler. Thromb. Vasc. Biol.* **1997**, *17*, 437−444.

(23) Dejager, S.; Mietus-Synder, M.; Pitas, R. E. Oxidized low-density lipoproteins bind to the scavenger receptor expressed by rabbit smooth muscle cells and macrophases. *Arterioscler. Thromb. Vasc. Biol.* **1993**, *13*, 371−378.

(24) Buege, J. A.; Aust, S. D. Microsomal lipid peroxidation. *Methods Enzymol.* **1978**, *52*, 302−310.

(25) Esterbauer, H.; Stiegal, G.; Puhl, H.; Rotheneder, M. Constinuous monitoring of in vitro oxidation of human low-density lipoprotein. *Free Radical Res. Commun.* **1989**, *6*, 67−75.

(26) Reid, V. C.; Mitchinson, M. J. Toxicity of oxidized low-density lipoprotein towards mouse peritoneal macrophases in vitro. *Atherosclerosis* **1993**, *98*, 17−24.

(27) Noguchi, N.; Niki, E. Apolipoprotein B protein oxidation in low-density lipoproteins. *Methods Enzymol.* **1994**, *233*, 490−494.

(28) Tolleson, W. H.; Doerge, D. R.; Churchwell, M. I.; Marques, M. M.; Roberts, D. W. Metabolism of biochanin A and formononetin by human liver microsomes in vitro. *J. Agric. Food Chem.* **2002**, *50*, 4783−4790.

(29) Garcez, W. S.; Martins, D.; Garcez, F. R.; Marques, M. R.; Pereira, A. A.; Oliveira, L. A.; Rondon, J. N.; Peruca, A. D. Effect of spores of saprophytic fungi on phytoalexin accumulation in seeds of frog-eye leaf spot and stem canker-resistant and susceptible soybean (*Glycine max* L.) cultivars. *J. Agric. Food Chem.* **2000**, *48*, 3662−3665.

(30) Venkateswarlu, S.; Panchagnula, G. K.; Guraiah, M. B.; Subbaraju, G. V. Isoaurostatin: total synthesis and structural revision. *Tetrahedron* **2005**, *61*, 3013−3017.

(31) Ingham, J. L.; Keen, N. T.; Mulheian, L. J.; Lyne, R. L. Inducibly formed isoflavonoids from leaves of soybean. *Phytochemistry* **1980**, *20*, 795−798.

(32) Al-Maharik, N.; Botting, N. P. A new short synthesis of coumestrol and its application for the syntheses of [6,6a,11a-$^{13}C_3$]coumestrol. *Tetrahedron* **2004**, *60*, 1637−1642.

(33) Lyne, R. L.; Mulheirn, L. J. Minor pterocarpinoids of soybean. *Tetrahedron Lett.* **1978**, *34*, 3127−3128.

(34) Rasool, N.; Khan, A. Q.; Ahmad, V. U.; Malik, A. A benzoquinone and a coumestan from *Psoralea plicata*. *Phytochemistry* **1991**, *30*, 2800−2803.

(35) Chauder, B. A.; Kalinin, A. V.; Taylor, N. J.; Snieckus, V. Directed metalation linked to transition metal catalyzed cascade reactions: Two total syntheses of plicadin, the alleged coumestan from *Psoralea plicata*. *Angew. Chem., Int. Ed.* **1999**, *38*, 1435−1438.

(36) Miyazawa, M.; Hisama, M. Antimutagenic activity of flavonoids from *Chrysanthemum morifolium*. *Biosci. Biotechnol. Biochem.* **2003**, *67*, 2091−2099.

(37) Hyun, J. W.; Chung, H. S. Cyanidin and malvidin from *Oryza sativa* cv. Heugjinjubyeo mediate cytotoxicity against human monocytic leukemia cells by arrest of G_2/M phase and induction of apoptosis. *J. Agric. Food Chem.* **2004**, *52*, 2213−2217.

(38) Havel, R. J.; Eder, H. A.; Bragdon, J. H. The distribution and chemical composition of ultracentrifugally separated lipoproteins in human serum. *J. Clin. Invest.* **1955**, *34*, 1345−1353.

Received for review October 1, 2005. Revised manuscript received January 25, 2006. Accepted February 1, 2006. This work is supported by a Grant (BioGreen 21 Project) from the Rural Development Administration, Korea.

JF052431C